

Scaling of angular distributions in multiparticle production

R. E. Gibbs

Department of Physics, Eastern Washington University, Cheney, Washington 99004

J. J. Lord and R. J. Wilkes

Department of Physics, University of Washington, Seattle, Washington 98195

(Received 23 December 1980)

We find that a simple scaling relation, $\langle \eta \rangle - \langle \eta \rangle_x = \delta\eta/R$, is consistent with data on multiparticle production from 30–400 GeV, where $\eta = -\ln \tan(\theta/2)$ is the pseudorapidity of produced fast particles, $\langle \eta \rangle_x$ is the average pseudorapidity of particles in excess of the hydrogen-target pseudorapidity distribution, and $R = \langle n_s \rangle / \langle n \rangle_H$ is the ratio of average multiplicity on a nuclear target to the average proton-proton multiplicity at equal energy. We find that the distance between the centroids of the hydrogen-target η distribution and the excess-particle distribution $\delta\eta = \langle \eta \rangle_H - \langle \eta \rangle_x = 1.74 \pm 0.06$ is independent of energy, target mass, and possibly projectile. This result implies that R increases with energy, and asymptotically is approximately proportional to ν , the number of collisions of the projectile.

I. INTRODUCTION

In the analysis of multiparticle production one can divide the final-state charged particles into two classes, those associated with an initial projectile-nucleon collision, and the “excess” particles associated with subsequent collisions within the struck nucleus. Experiments typically measure the pseudorapidity $\eta = -\ln \tan(\theta/2)$ instead of the true rapidity $y = 0.5 \ln[(E + p_z)/(E - p_z)]$. In the energy range from 30 to 400 GeV we find that the average pseudorapidity of these excess particles, $\langle \eta \rangle_x$, differs from that in hydrogen, $\langle \eta \rangle_H$, by the fixed amount $\delta\eta = \langle \eta \rangle_H - \langle \eta \rangle_x = 1.74$ independent of the primary energy, the mass of the target nucleus, and the number of charged secondaries. It is possible that $\delta\eta$ is independent of the projectile as well. This result implies that R increases with energy, and asymptotically is approximately proportional to ν , the number of intranuclear collisions of the projectile. Andersson, Otterlund, and Stenlund¹ have reached a similar conclusion based on an analysis of multiplicity data.

This result is consistent with results presented previously,² outlining an improved method of estimating the energies of cosmic-ray interactions from the angular distributions.

II. DETERMINING $\langle \eta \rangle_x$

Several models of nuclear cascading assume that the excess particles have an η distribution whose location on the η axis is fixed with respect to the distribution for collisions in hydrogen.^{3–6} Such a situation is shown schematically in Fig. 1, where the first collision produces $\langle n \rangle_H$ particles and subsequent collisions produce $\langle n \rangle_x$ particles.

Then

$$\langle \eta \rangle = \frac{\langle n \rangle_H \langle \eta \rangle_H + \langle n \rangle_x \langle \eta \rangle_x}{\langle n \rangle_H + \langle n \rangle_x}. \quad (1)$$

We define $\delta\eta = \langle \eta \rangle_H - \langle \eta \rangle_x$ and $\langle n_s \rangle = \langle n \rangle_H + \langle n \rangle_x$. Then Eq. (1) becomes

$$\langle \eta \rangle = \langle \eta \rangle_x + \frac{\langle n \rangle_H}{\langle n_s \rangle} \delta\eta. \quad (2)$$

One can then plot $\langle \eta \rangle$ versus $1/\langle n_s \rangle$ and determine the value of $\langle \eta \rangle_x$ from the intercept of the resulting straight line. This has been done by Dar *et al.*⁸ for p -emulsion collisions at 200, 300, and 400 GeV. In Fig. 2 we have plotted data in this manner from several experiments^{6–8} in the energy range 30–400 GeV using various projectiles and target nuclei. The values for $\langle n \rangle_H$ given in Ref. 8 were determined from a subtraction of CH_2 and carbon-target data. Since these values in some cases differ significantly from the equivalent bubble-chamber results, in making

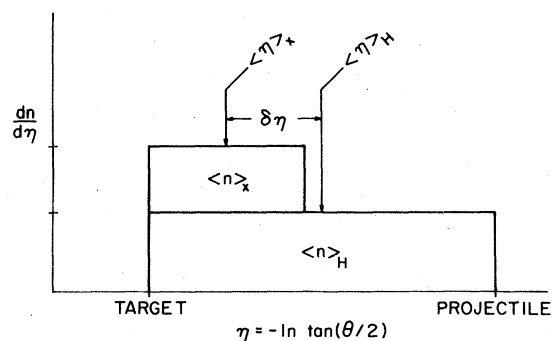


FIG. 1. An idealized pseudorapidity distribution showing the quantities used in the text.

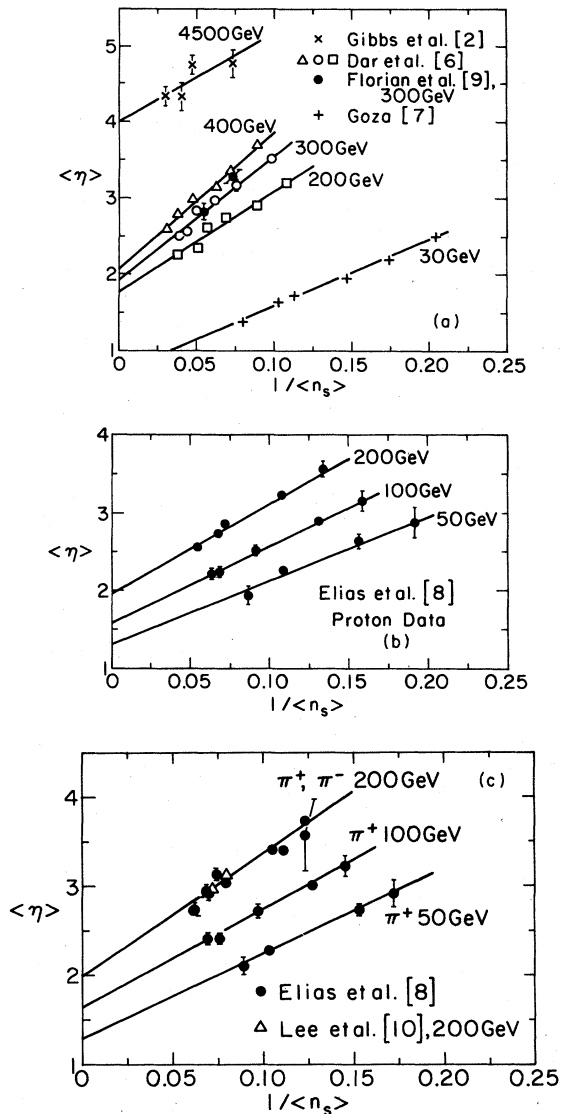


FIG. 2. Plots of Eq. (2) $\langle \eta \rangle$ vs $\langle n_s \rangle^{-1}$ for several experiments: (a) proton-emulsion data (Refs. 2, 6, and 7), with the data for each energy binned according to the number of heavily ionizing tracks present; also shown are the pure-target data of Ref. 9; (b) proton-nucleus data from Ref. 8; (c) pion-nucleus data (Refs. 8 and 10).

our plots we have substituted the values determined by Albin *et al.*¹¹ from fits to a compilation of world data. We have also plotted our data for 300-GeV protons⁹ and 200-GeV π^- (Ref. 10) striking tungsten and chromium grains embedded in photographic emulsion. Finally we include cosmic-ray data analyzed by our group in 1974.² It should be noted that in the emulsion-target data^{2,6,7} the identity of the struck nucleus is not known, and is inferred from the number of heavily ionized ($\beta < 0.7$) tracks produced.

Equation (2) provides two methods for determining $\delta\eta$. First, the intercept of the linear fit gives $\langle \eta \rangle_x$, which can be subtracted from $\langle \eta \rangle_H$. For example, $\langle \eta \rangle_H = 3.9$ for 300-GeV proton-proton interactions,¹² and thus $\delta\eta = 2.0$; however, accurate values of $\langle \eta \rangle_H$ are not available for all projectiles and energies considered here. Second, the slope can be divided by $\langle \eta \rangle_H$; since reliable values for the hydrogen-target multiplicities can be obtained from Ref. 11, we have used this method in this paper. For the example given above, the results of the two methods are equivalent within errors.

Table I lists the results of fits to Eq. (2) for each data sample. The values of χ^2 indicate that the data are consistent with linearity. This implies that $\langle \eta \rangle_x$ is independent of n_s and therefore of ν , the number of secondary collisions in the struck nucleus, which in turn implies that $\langle \eta \rangle_x$ is independent of the mass of the struck nucleus.

The table indicates that the emulsion data yield smaller values for the intercept and larger slopes than the corresponding data from Ref. 8. This is apparently due to systematic differences in experimental technique, including the following factors.

(1) In emulsion the angle of each track is measured individually to determine η , while in counter experiments η is averaged over angular bins defined by the apparatus.

(2) Elias *et al.*⁸ have removed coherent events from the sample, a procedure not routinely carried out in emulsion experiments.

(3) Systematic corrections for trigger and counter inefficiencies are not required in emulsion experiments; in particular, emulsion has 4π sensitivity and detects all backward tracks with the same efficiency as forward tracks.

(4) The emulsion technique counts all particles of $\beta \geq 0.7$ while the experiment of Ref. 8 included $\beta > 0.85$.

Fortunately, these differences are not serious enough to obscure our basic conclusions.

The last column of the table gives $\delta\eta$ as determined from the slopes of the linear fits. Discounting the differences between experimental techniques, it is clear that $\delta\eta$ is essentially independent of both primary energy and projectile.

In Fig. 2 we show a representative sample of plots from the data of Table I. Figures 2(a) and 2(b) illustrate the systematic differences between the emulsion data and those of Ref. 8. In Fig. 2(c) we find that our data for 200-GeV π^- in tungsten and chromium is quite compatible with

TABLE I. Weighted fits to Eq. (2). Values of $\langle n \rangle_H$ are taken from Ref. 11.

E (GeV)	Projectile	Intercept $\langle \eta \rangle_x$	Slope $\langle n \rangle_H \delta \eta$	χ^2/DF	$\delta \eta = \frac{\text{slope}}{\langle n \rangle_H}$
Emulsion data (Refs. 2, 6, 7)					
30	p	0.72 ± 0.04	8.6 ± 0.3	1.2	1.90 ± 0.07
200	p	1.76 ± 0.05	13.3 ± 0.6	4.0	1.77 ± 0.08
300	p	1.92 ± 0.05	16.5 ± 0.8	3.8	1.99 ± 0.09
400	p	2.06 ± 0.03	18.1 ± 0.5	2.8	2.04 ± 0.05
4500	p	4.00 ± 0.20	12.0 ± 5.0	1.7	
Data from Ref. 8					
50	p	1.30 ± 0.20	8.5 ± 1.5	0.7	1.60 ± 0.30
100	p	1.56 ± 0.10	10.3 ± 0.9	0.1	1.63 ± 0.14
200	p	1.94 ± 0.08	12.2 ± 0.9	0.7	1.62 ± 0.12
50	κ^+	1.52 ± 0.46	8.2 ± 3.5	0.5	1.40 ± 0.60
100	κ^+	1.45 ± 0.16	11.9 ± 1.9	0.9	1.68 ± 0.27
50	π^+	1.30 ± 0.14	9.4 ± 1.2	0.1	1.60 ± 0.20
100	π^+	1.63 ± 0.11	10.9 ± 1.0	0.3	1.58 ± 0.15
200	π^+	2.00 ± 0.13	13.5 ± 1.30	2.3	1.66 ± 0.16
200	π^-	1.97 ± 0.11	13.1 ± 1.3	0.8	1.61 ± 0.16
200	\bar{p}	1.60 ± 0.47	15.0 ± 5.8	0.9	1.94 ± 0.72

the 200-GeV π^- data of Elias *et al.*⁸ For the cosmic-ray proton data of Fig. 2(a) the slope does not seem large enough for the calculated energy. However, we will show shortly that the intercept, which is much more accurately determined, is consistent with this analysis.

In Fig. 3 we plot $\langle \eta \rangle_x$ versus $\ln E$ for the primary proton data. Dar *et al.*⁶ have noted previously that $\langle \eta \rangle_x$ is consistent with linearity in $\ln E$ with a slope of 0.5 for data on p -emulsion collisions of 200, 300, and 400 GeV. As can be seen from Fig. 3, the sets of emulsion data^{6,7} and the counter data⁸ taken separately each provide an excellent fit to a straight line with slope 0.5, but the two fits yield intercepts which differ significantly due to the systematics discussed above. A weighted

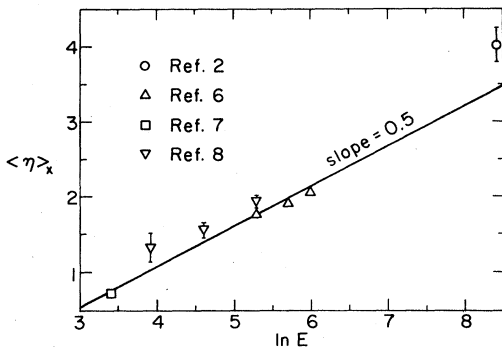


FIG. 3. Plot of $\langle \eta \rangle_x$ vs $\ln E$ for proton primary data in emulsion and the experiments of Elias *et al.* (Ref. 8). The cosmic-ray point is plotted for comparison but is not included in the fit.

average of the two fits yields the parameter values

$$\langle \eta \rangle_x = -(0.97 \pm 0.11) + (0.51 \pm 0.02) \ln E \quad (3)$$

(for E in GeV), where the rather large error on the intercept reflects the systematic error. The cosmic-ray value² is included for comparison but was not part of the fit.

Dar *et al.*⁶ have shown from kinematics that for proton-proton collisions

$$\langle \eta \rangle_H = 0.5 \ln E - 0.5 \ln(m_p/2) + \Delta, \quad (4)$$

where $\Delta = 0.45$ accounts for the difference between $\langle \eta \rangle$ and the average true rapidity $\langle y \rangle$. Combining (3) and (4) we find

$$\begin{aligned} \delta \eta &= \langle \eta \rangle_H - \langle \eta \rangle_x \\ &= -(0.01 \pm 0.02) \ln E + (1.80 \pm 0.11) \\ &= 1.80 \pm 0.11 \end{aligned} \quad (5)$$

essentially independent of energy.

In Fig. 4 we plot $\langle \eta \rangle_x$ versus $\ln E$ for the data of Elias *et al.*⁸ for several different primaries. The best fit is

$$\langle \eta \rangle_x = (-0.62 \pm 0.40) + (0.48 \pm 0.08) \ln E. \quad (6)$$

This is again consistent with a slope of 0.5, and suggests that $\delta \eta$ is independent of projectile, in agreement with the data of Table I.

Since $\delta \eta$ is a constant, Eq. (2) can be written

$$\langle \eta \rangle - \langle \eta \rangle_x = \delta \eta / R, \quad (7)$$

where $R = \langle n_s \rangle / \langle n \rangle_H$. Thus, the family of straight lines of Fig. 2 can now be plotted as a single straight line. In Fig. 5 we replot the data of Fig.

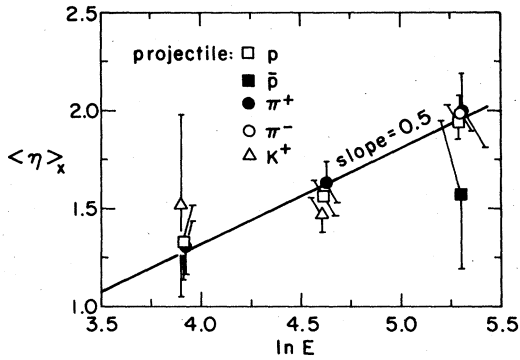


FIG. 4. Plot of $\langle \eta \rangle_x$ vs $\ln E$ for the data of Elias *et al.* (Ref. 8), including p , \bar{p} , π^+ , and K^+ projectiles.

2 in terms of Eq. (7). Error bars in this figure include errors in both $\langle \eta \rangle$ and $\langle \eta \rangle_x$.

In Fig. 5 we have included our data for p -tungsten and p -chromium collisions at 300 GeV and π^- -tungsten and π^- -chromium collisions at 200 GeV. To do so we have assumed that the $\langle \eta \rangle_x$ values for these data are the same as for the corresponding energy in p -emulsion experiments. This assumption is reasonable in view of the results shown in Figs. 2(a) and 2(c) and from consideration of the experimental procedure involved. Small grains of the target material were placed in the photographic emulsion and then normal emulsion analysis techniques were used.

A linear fit to the data of Fig. 5 gives $\delta\eta = 1.74 \pm 0.06$ which is in agreement with the value obtained in Eq. 5.

III. COMPARISON TO THEORY

We currently have no detailed theory of intranuclear cascade processes. However, a number of phenomenological models have been very useful for analyzing data. Those models³⁻⁵ which assume that the excess-particle rapidity distribution is some constant fraction of the proton-proton rapidity distribution are inconsistent with the energy independence of $\delta\eta$.

The collective tube model⁶ is consistent with an energy-independent $\delta\eta$, but in this model $\delta\eta$ depends on ν , the number of collisions, and therefore, on the target nucleus and n_s . This can be easily shown in the following way. In this model⁶ the average rapidity for proton-nucleus collisions is

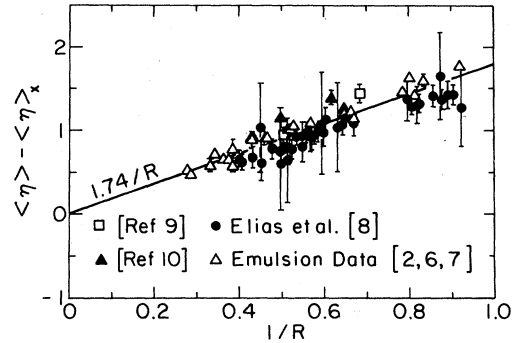


FIG. 5. Data of Fig. 2, replotted in terms of $\langle \eta \rangle - \langle \eta \rangle_x$ vs $1/R$.

$$\langle y \rangle = 0.5 \ln(2E/m_p) - 0.5 \ln(\nu). \quad (8)$$

Since $\langle y \rangle$ differs from $\langle \eta \rangle$ by a constant term $\Delta = 0.45$, and since $\nu = 1$ corresponds to $\langle y \rangle_H$, we can write

$$\langle \eta \rangle = \langle \eta \rangle_H - 0.5 \ln(\nu). \quad (9)$$

Comparing this to Eq. (2) we find

$$\delta\eta = \frac{R}{R-1} (0.5 \ln \nu). \quad (10)$$

Whether one chooses $R = \frac{1}{2} + \frac{1}{2}\bar{\nu}$ or the asymptotic form of Andersson *et al.*,¹ $R = 0.12 + 0.9\bar{\nu}$, $\delta\eta$ depends on ν , and has a value for small ν of about 1.0.

IV. IMPLICATIONS

The observed result is that $\delta\eta$ is fixed, or alternatively, that $\langle \eta \rangle_x$ grows with energy at the same rate as $\langle \eta \rangle_H$. This implies that each secondary collision contributes an average number of particles that is less than $\langle n \rangle_H$ by an energy-independent constant, assuming that (a) the height of the η_x distribution is equal to that of the η_H distribution, and (b) the tails of the η_H and η_x distributions coincide at the low- η end, as suggested in Fig. 1. Thus, asymptotically the ratio $R = \langle n_s \rangle / \langle n \rangle_H$ must be proportional to ν , the number of collisions. This is essentially the same conclusion reached by different means by Andersson *et al.*,¹ who find that asymptotically $R = 0.12 + 0.9\bar{\nu}$.

ACKNOWLEDGMENTS

This work was supported by DOE Contract No. EY765062225/TA27. R.E.G. was supported by the National Science Foundation.

- ¹B. Andersson, I. Otterlund, and E. Stenlund, Phys. Lett. 84B, 469 (1979).
- ²R. E. Gibbs, J. R. Florian, L. D. Kirkpatrick, J. J. Lord, and J. W. Martin, Phys. Rev. D 10, 783 (1974).
- ³K. Gottfried, Phys. Rev. Lett. 32, 957 (1974).
- ⁴P. M. Fishbane and J. S. Trefil, Phys. Rev. D 9, 168 (1974).
- ⁵P. M. Fishbane and J. S. Trefil, Phys. Lett. 51B, 139 (1974).
- ⁶A. Dar, I. Otterlund, and E. Stenlund, Phys. Rev. D 20, 2349 (1979).
- ⁷E. R. Goza, thesis, University of Washington, 1962 (unpublished).
- ⁸J. E. Elias, W. Busza, C. Halliwell, D. Luckey, P. Swartz, L. Votta, and C. Young, Phys. Rev. D 22, 13 (1980).
- ⁹J. R. Florian, M. Y. Lee, J. J. Lord, J. W. Martin, R. J. Wilkes, R. E. Gibbs, and L. D. Kirkpatrick, Phys. Rev. D 13, 558 (1976).
- ¹⁰M. Y. Lee, J. J. Lord, and R. J. Wilkes, Phys. Rev. D 19, 55 (1979).
- ¹¹E. Albini, P. Capiluppi, G. Giacomelli, and A. M. Rossi, Nuovo Cimento 32A, 101 (1976).
- ¹²F. Dao *et al.*, Phys. Lett. 45B, 73 (1973).